# Comparison of two simple high-frequency earthing electrodes

R.L. Stoll, G. Chen and N. Pilling

**Abstract:** Lightning strikes on high-voltage transmission lines may create hazardous touch potentials on adjacent substation equipment and damage control equipment. When designing suitable substation earthing electrodes to overcome this problem and safely dissipate the transient fault currents to ground, it is essential to consider the behaviour of the current flow. The steady-state frequency equivalent to a lightning strike is at least 0.25 MHz, which corresponds to a current skin depth $\delta$ of about 10 m in homogeneous soil of conductivity 0.01 S/m. This surface effect causes the impedance of an electrode system to be considerably larger than the power-frequency resistance. Thus a dedicated electrode is normally placed in parallel with the low-frequency earthing system, usually taking the form of a simple vertical rod of copper-coated steel about 5 m long. The work presented suggests that a long rod is not ideal for the purpose. Using a relatively simple numerical finite-difference procedure it has been found that a flat disc electrode parallel to the surface of the ground achieves a significant improvement over the performance of a vertical rod. Both rod and disc have been solved in the frequency domain, but the rod has also been analysed in time-stepping form so that the peak voltage for a given imposed current can be compared with that deduced from the equivalent steady-state complex impedance.

## 1 Introduction

High-voltage substations are provided with secure earthing systems in the form of a horizontal grid or lattice of copper rods about 0.5 m below the surface, often combined with vertical driven rods connected to some of the intersecting nodes, particularly around the edges of the grid. This system is designed to provide a low-resistance path for power-frequency fault currents radiating out towards a zero-potential hemisphere of very large radius (the so-called 'true earth plane'). The major part of this ohmic resistance occurs close to the earthing system and can be reduced by increasing the dimensions of the grid and/or adding more vertical rods. However, the latter must be sufficiently far apart to avoid deterioration of their individual effectiveness due to mutual interference. In contrast, the size of the true earth hemisphere assumed for the purpose of calculation is not important. For example, the DC resistance of a shell of homogeneous soil of conductivity 0.01 S/m carrying a uniformly distributed and radially directed current between a hemisphere of radius 1 km and infinity is only about 16 m$\Omega$.

When considering the requirement for protection against high-frequency transient faults, such as those caused by lightning strikes on nearby transmission lines, a system designed to handle power-frequency fault currents may be unable to prevent hazardous touch and step potentials or damage to control equipment.



*IEE Proceedings* online no. 20040013

doi:10.1049/ip-gtd:20040013

Paper first received 11th September 2002 and in revised form 15th July 2003. Online publishing date: 13 February 2004

R.L. Stoll and G. Chen are with the Department of Electronics and Computer Science, University of Southampton, UK

N. Pilling is with the National Grid Company, UK

First, the steel structural components used to support some substation equipment are not generally suitable for carrying high-frequency fault currents into the earthing system due to the very high surface current density (resulting from the well-known eddy-current skin effect). At 0.5 MHz, for example, the internal impedance of a steel angle section can be up to two orders of magnitude higher than at 50 Hz, so that a large current may produce a dangerous touch potential. The use of copper straps connecting equipment directly to the below-ground electrodes is therefore advisable.

Secondly, the behaviour of the fault current within the ground needs to be considered. It is well known that the skin-depth parameter in a nonmagnetic conducting material is defined as $\delta = 1/\sqrt{\pi f \sigma \mu_0}$ [1], so that for homogeneous soil of conductivity $\sigma = 0.01$ S/m have $\delta = 5033/\sqrt{f}$. Given that the steady-state frequency usually taken to represent a lightning strike is in the range 0.25 to 0.5 MHz, $\delta$ varies between 10.1 and 7.12 m. The current density decays exponentially with distance from the surface according to the complex factor $\exp\{(1+j)y/\delta\}$ [1], and so the major portion of the current flows within a surface layer of depth $3\delta$, i.e. up to about 30 m. Thus a short distance from the injection point the current will have established a flow pattern of relatively shallow depth that is almost entirely parallel to the surface and directed away from the axis of symmetry.

Under homogeneous soil conditions this surface effect will cause the impedance of any electrode system (a reactive component is now involved) to be larger than the low-frequency resistance. Thus a dedicated electrode is often used in parallel with the low-frequency system, usually consisting of a long vertical driven rod of copper-coated steel with a copper strap connection reaching directly up to the apparatus to be protected. The rod may be typically 5 m in length and 16 mm in diameter. However, the work presented in this paper suggests that a long rod is not ideal

for the purpose, the reason being that the current will tend to leave the surface of the rod in a way that mirrors the exponential form of the skin effect. Indeed a 30 m rod would inject current into the surrounding soil in an almost exact one-dimensional flow pattern. The current density near the top of the rod will not only be very high but also restricted to a small surface area, to the detriment of the resulting impedance that is strongly influenced by the near-field region. The rapidly decreasing benefit of lengthening a vertical rod is well illustrated by the analysis described in Section 2, which has been used to show that an increase in length from 3 to 4 m decreases the impedance by about 13%, whereas from 5 to 6 m only achieves a 6% reduction.

There is nothing that can be done to avoid the skin-dominated current flow further from the electrode, but it would be useful to find an electrode shape that reduces the tendency to establish a strong skin-dominated regime close to the device. Using a relatively simple numerical finite-difference procedure, it has been found that a flat disc electrode parallel to the surface of the ground achieves a significant improvement over the performance of a vertical rod, due only in part to the increased surface area of the conductor. The reactive component of the impedance is lower, and, unlike the rod, increasing the major dimension (radius) of the disc does not increase its reactance.

When comparing the performance of a disc and rod, one possibility is to select a disc radius that yields the same DC resistance as a 5 m rod, namely 21.6 Ω in soil of conductivity 0.01S/m. For ease of calculation, the simpler position for a disc is on the ground surface where current exits only from its lower face. In this position the DC resistance is given by $1/4a\sigma$, where $a$ is the radius of the disc, leading to $a = 1.16$ m. Thus we investigate how surface discs with radii in the range 1 to 1.5 m compare with a standard rod of length 5 m. In practice a disc would be buried about 0.5 m below the surface, thus lowering the impedance slightly.

The analysis is based on the numerical finite-difference method because the geometry of the two electrodes is simple. This choice is one of convenience and not intended to suggest that the method is superior to other well-established techniques [2] such as finite elements for which commercial software is readily available, e.g. the Opera suite of computer programs produced by Vector Fields [3]. The only advantage of the method of finite differences is that the program is easy to construct when the geometry is simple, and, if desired, displacement effects can be added very easily to the main diffusion process, see (1). However, displacement current is not significant in typical soil conditions below about 1 MHz. The defining diffusion equation can be solved in either the frequency domain using complex variables, or in the time domain by time-stepping.

A lightning discharge is conventionally represented in terms of an equivalent steady-state frequency so that the ground impedance of the electrode can be determined. The latter parameter is of vital interest because, for a given fault current, it dictates the potential rise that will be experienced by the connected apparatus. Typical rise times for the current pulses associated with lightning are in the range 0.5 to 1 $\mu$s, leading to equivalent periodic times of between 2 and 4 $\mu$s, and frequencies from 0.5 to 0.25 MHz.

An important practical effect neglected in the present work is soil breakdown due to the very high electric field that may occur at the electrode surface as the transient fault current reaches its peak. The soil ionisation gradient is usually taken to be between 300 and 400 kV/m [4] and when the surface electric field exceeds this threshold the electrode is effectively surrounded by a sheath of soil of relatively high conductivity whose thickness varies with time as the electric field changes. Geri [4] models the phenomenon by increasing the diameter of the rods forming the electrode system. A vertical rod electrode subjected to a massive discharge will almost certainly experience soil breakdown near the ground surface where the current density is higher, whereas the disc is less likely to do so because of the greater surface area. Thus, in the present comparison, where the soil is assumed to be a linear homogeneous material, the real resistance of the vertical rod will be lower than the value calculated if the effective rod diameter near the ground surface has increased due to ionisation. However, the intention of the work described here is not to model the electrodes in great detail but to reveal an interesting, and initially unexpected, feature regarding the difference between the two reactive components of impedance mentioned earlier. Furthermore detailed analysis of a buried disc in a practical situation, e.g. modelling soil nonlinearity, can be undertaken at a later date.

Both rod and disc have been solved in the frequency domain, but the rod has also been analysed in time-stepping form so that the peak transient voltage for a given current impulse can be compared with that deduced from the equivalent steady-state complex impedance.

## 2 Numerical method for steady-state solution

Both rod and disc have axial symmetry so that the solution can be found in terms of the single circumferential component of magnetic field $H_\theta$ in a cylindrical ($r$, $\theta$, $z$) co-ordinate system, with the z-axis forming the axis of symmetry; $H_\theta$ is a function of $r$ and $z$ only and on the surface of the ground ($z = 0$) $H_\theta = I/2\pi r$ where $I$ is the peak injected current. The other boundary conditions can be assumed to be as shown in Fig. 1, where the problem has been inverted for convenience. The current skin effect will cause $H_\theta$ to tend to zero at a large depth $z = d$, where $d$ can be taken as approximately four times the skin depth $\delta$. On the surface of the rod $r = a$ the electric field component $E_z$ is required to be zero because the electrode is assumed to be infinitely conducting. If the current leaving the small tip of the electrode is neglected, $H_\theta = 0$ on the section of the boundary $r = a$, $l < z < d$. At some distance $r = c$ from the axis of symmetry (where $c$ is typically about 30 m), the current flow has one-dimensional form and is entirely radial, leading to the condition $E_z = 0$.

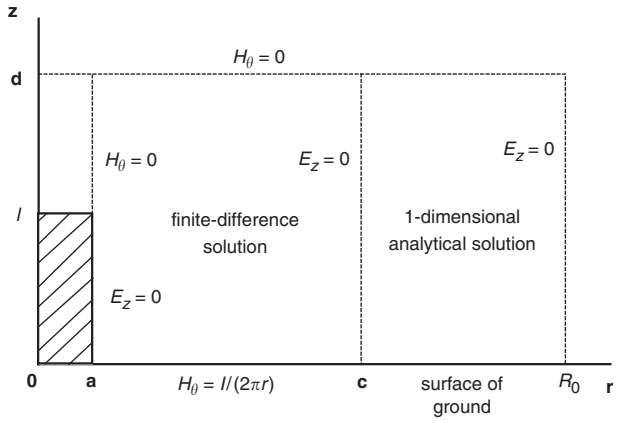


**Fig. 1** *Outline of two field regions and boundary conditions, the first to be solved numerically and the second analytically*

In problems of this type the partial-differential equation for $H_\theta$ (derived from Maxwell's equations) can be simplified by the substitution $H = rH_\theta$ which then results in the

modified equation

$$\frac{\partial^2 H}{\partial r^2} - \frac{1}{r}\frac{\partial H}{\partial r} + \frac{\partial^2 H}{\partial z^2} = -\gamma^2 H \tag{1}$$

where $\gamma^2 = \omega^2\varepsilon_0\varepsilon_r\mu_0 - j\omega\sigma\mu_0 = -j\omega\mu_0(\sigma + j\omega\varepsilon_0\varepsilon_r) = -j\omega\mu_0\beta$. The term containing the soil permittivity $\varepsilon_0\varepsilon_r$ is included for completeness but is not significant in value until the frequency approaches 1 MHz.

One of Maxwell's field equations relates **E** and **H** in complex form

$$\text{curl}\,\boldsymbol{H} = (\sigma + j\omega\varepsilon_0\varepsilon_r)\boldsymbol{E} = \beta\boldsymbol{E}$$

Thus the electric field components can be expressed as

$$\beta E_r = -r^{-1}\partial(rH_\theta)/\partial z = -r^{-1}\partial H/\partial z \tag{2}$$

$$\beta E_z = \partial H_\theta/\partial r + H_\theta/r = r^{-1}\partial H/\partial r \tag{3}$$

When $E_z = 0$, (3) simplifies to $\partial H/\partial r = 0$, and the boundary conditions in terms of the modified field component $H$ or its normal derivative are shown in Fig. 2. Using centre differences, (1) can be written in finite-difference form as

$$\frac{H_{i,j+1} - 2H_{i,j} + H_{i,j-1}}{(\Delta z)^2} + \frac{H_{i+1,j} - 2H_{i,j} + H_{i-1,j}}{(\Delta r)^2} - \frac{H_{i+1,j} - H_{i-1,j}}{2r_i\Delta r} + \gamma^2 H_{i,j} = 0 \tag{4}$$

where Fig. 2 has been overlaid by a rectangular grid or mesh with cells of dimension $\Delta r \times \Delta z$. Each node of the grid has a unique address $(i, j)$ where $r_i = a + (i-1)\Delta r$ and $z = (j-1)\Delta z$, the corner point $r = a$, $z = 0$ having the address (1, 1).

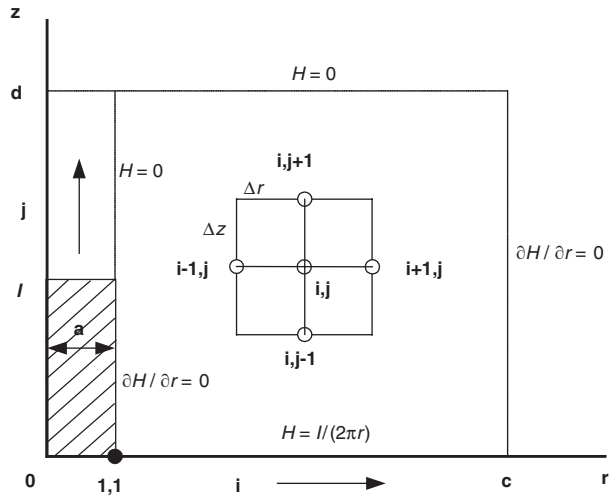


**Fig. 2** *Finite-difference region with modified boundary conditions; grid notation is also shown*

In the successive over-relaxation (SOR) method the grid is scanned by columns starting at node (1,1) to progressively refine $H_{i,j}$ in terms of the four neighbouring values. SOR uses updated values as soon as they are available and so during the $(k+1)$th iteration or scan

$$H_{i,j}^{(k+1)} = C_E H_{i+1,j}^{(k)} + C_W H_{i-1,j}^{(k+1)} + C_{NS}\{H_{i,j+1}^{(k)} + H_{i,j-1}^{(k+1)}\} \tag{5}$$

where $C_E = (\Delta z)^2(2r_i - \Delta r)D^{-1}$

$C_W = (\Delta z)^2(2r_i + \Delta r)D^{-1}$

$C_{NS} = 2r_i(\Delta r)^2 D^{-1}$

and $D = 2r_i[2\{(\Delta r)^2 + (\Delta z)^2\} - (\Delta r)^2(\Delta z)^2\gamma^2]$

The change in the value of $H_{i,j}$ that is taking place is known as the residual or displacement

$$R_{i,j} = H_{i,j}^{(k+1)} - H_{i,j}^{(k)} \tag{6}$$

The SOR technique, as its name implies, is to enhance or accelerate the direction of this change by a factor $\alpha$. Thus the new value of $H_{i,j}$ is given by

$$H_{i,j}^{(k+1)} = H_{i,j}^{(k)} + \alpha R_{i,j} \tag{7}$$

In practice, because $H_{i,j}$ is complex, it is found more effective to have a complex acceleration factor $a$ of the form $a - jb$, where $a < 2$ and $b \ll a$. A typical value for a large grid of about $10^6$ nodes is $1.98 - j0.002$ but it is advantageous to improve the estimate of $\alpha$ during the iterative process. A useful technique is given by Stoll [5], based on the original real-number method of Carre [6].

The Dirichlet boundary conditions on $z = 0$, $z = d$, and $r = a$ $(z \geq l)$ in Fig. 2 remain fixed during the iterative process. However, where the Neumann condition $\partial H/\partial r = 0$ prevails the boundary nodes have to be included during each scan. For example, on $r = c$, the simple centre-difference formula requires that the value of $H$ at the imaginary node just outside the boundary is equal to the value just inside, i.e. $H_{i+1,j} = H_{i-1,j}$. This substitution is made in (5) for these boundary nodes.

The solution is assumed to have converged to the required steady-state set of complex values of $H_{i,j}$ when the maximum residual (6) detected during a given scan of the mesh is less than some value specified in the data; a quantity determined by numerical experiment.

Following satisfactory convergence, the impedance is determined by integrating $E_r$ along the surface of the ground from the rod to the radius of the 'true earth' hemisphere, which is here taken to be $R_0 = 2000$ m.

The outer radius $c$ of the inner zone where the finite-difference method has been applied is at sufficient distance from the rod for the one-dimensional skin effect to have fully formed. It is therefore easy to determine the contribution of the outer zone to the integral of $E_r$ because the electric field is entirely radially directed. Thus, the flux crossing a thin circular ribbon of radius $c$ and depth $\delta z$ is $2\pi c\delta z E_c$, where $E_c$ is the value of $E_r$ at $r = c$. But the same flux will cross a similar ribbon of any radius $r$ within the outer zone $c \leq r \leq R_0$. Thus $rE_r = cE_c$ and the integral reduces to

$$\int_c^{R_0} E_r dr = cE_c \int_c^{R_0} \frac{dr}{r} = cE_c \ln(R_0/c)$$

The contribution of the outer zone to the impedance is therefore given by

$$Z_o = cE_c \ln(R_0/c)/I \tag{8}$$

where $I$ is the peak fault current injected by the rod. For the inner region $(0 < r < c)$ $E_r$ must be computed at each surface node. Equation (2) indicates that this process requires $\partial H/\partial z$ at each point. A formula for the derivative of an end (surface) point is given by Burden and Faires [7],

and so (2) yields

$$E_r|_{i,1} = \frac{1}{12\beta\Delta z r_i}(25H_{i,1} - 48H_{i,2} + 36H_{i,3} - 16H_{i,4} + 3H_{i,5}) \quad (9)$$

where $H_{i,1}$ is the constant boundary value $I/2\pi$. The integral of $E_r$ over the range $0 \leq r \leq c$ is obtained by Gregory's formula, which can be applied to either an odd or even number of equally spaced values. The inner zone impedance $Z_i$ then follows by dividing the integral by the injected current and the total impedance is simply $Z_i + Z_o$.

If the rod is replaced by a disc with its lower surface in contact with the ground, the solution process is almost identical. The left-hand boundary in Fig. 2 is now the axis of symmetry $r = 0$ where $H = 0$. On the ground surface $z = 0$, the condition $E_r = 0 = \partial H/\partial z$ is imposed over the conducting surface $0 < r < a$ (where $a$ is now the radius of the disc), with $H = I/2\pi$ for $r \geq a$ as before.

## 3 Steady-state results

The standard vertical rod of 5 m length and 8 mm radius presents a below-ground impedance of $29.18 + j12.41$ at 0.25 MHz rising to $33.43 + j20.11$ at 0.5 MHz. The magnitudes are 31.71 and 39.01Ω, respectively. The soil conductivity has been taken as 0.01 S/m with a relative permittivity of 10, although the displacement current is almost negligible below 1 MHz.

Table 1 lists the impedance at two frequencies of surface discs having radii between 1.0 and 1.5 m, this range having been selected in view of the fact that a disc of radius 1.16 m has a DC resistance equal to that of the rod (21.6 Ω). However, Fig. 3 illustrates wider range of disc size at 0.25 MHz, where it can be seen that a radius of 1.05 m gives the same resistance as the rod but with the advantage of about 3.5 Ω less reactance; a 28% decrease. At the higher frequency of 0.5 MHz this reactance advantage is found to improve to 34%. The disc reactance appears to be virtually independent of radius over the range considered; some of the small variation shown in Table 1 being due to numerical discretisation error.

The reason for the lower and constant values of disc reactance must lie in the fact that the long rod facilitates the establishment of the one-dimensional skin behaviour closer to the electrode than occurs with the disc. In a fully established skin pattern it is well known that the resistive and reactive components are equal.

Figure 4 shows the way in which the surface electric field decays rapidly from the surface of a 5 m rod and the edge of a disc of 1 m radius when a peak current of 1000A is injected at 0.25 MHz. The electric field, having the units V/m, is equivalent to the step potential. At this frequency the magnitude of the electric field is considerably higher close to the edge of the disc, although in practice the latter would be buried to a depth of at least 0.5 m. At distances greater than 3 m from the electrodes the curves are almost identical. Even with a fault current of only 1000A the ground surface could be hazardous within about 8 m of the electrodes. High-voltage electrodes should therefore be placed as far from the perimeter fence of the substation as possible, and appropriate areas within the compound covered by layers of insulation.

## 4 Transient solution

When studying the same problem under a transient current pulse, the magnetic field component $H$ in (1) is no longer complex but a function of time, and the right-hand side of the equation must be replaced by $\sigma\mu_0\partial H/\partial t$. This is a diffusion equation (with no displacement term) and can be solved by a finite-difference time-stepping method.

In the simple explicit time-stepping algorithm $\partial H/\partial t$ at node $i, j$ is expressed by the forward difference approximation

$$(H_{i,j,k+1} - H_{i,j,k})/\Delta t$$

where the time at step $k$ is given by $t = k\Delta t$. The space derivatives in (1) are expressed in the usual way in terms of the nodal values at step $k$. Thus one new value at step $k+1$ is expressed in terms of four known values at step $k$, leading to the name explicit. Unfortunately this algorithm is only stable for very small time increments $\Delta t$ and therefore not efficient in computation time. Although it is possible to move to the relative complexity of an implicit method, where all the new values at step $k+1$ have to be computed in one operation, there is an explicit and unconditionally stable scheme that was devised by Dufort and Frankel [8]. However, the algorithm may be subject to truncation errors unless

$$(\Delta t/\Delta x) \ll \sqrt{(\sigma\mu_0)} \quad (10)$$

where $\Delta x$ is the smaller of $\Delta r$ and $\Delta z$. The Dufort–Frankel equation can be derived from the simple explicit equation by simply replacing $H_{i,j,k}$ by the average of the $H_{i,j}$ values at $k-1$ and $k+1$ to yield an equation of the following form:

$$H_{i,j,k+1} = c_e H_{j+1,j,k} + c_w H_{i-1,j,k} + c_{ns}(H_{i,j+1,k} + H_{i,j-1,k}) + c_c H_{i,j,k-1} \quad (11)$$

$$\text{where } c_e = (\Delta r)^{-2}\{1 - 0.5(\Delta r/r_i)\}d^{-1}$$
$$c_w = (\Delta r)^{-2}\{1 + 0.5(\Delta r/r_i)\}d^{-1}$$
$$c_{ns} = (\Delta z)^{-2}d^{-1}$$
$$c_c = \{0.5\sigma\mu_0(\Delta t)^{-1} - (\Delta r)^{-2} - (\Delta z)^{-2}\}d^{-1}$$
$$\text{and } d = \{0.5\sigma\mu_0(\Delta t)^{-1} + (\Delta r)^{-2} + (\Delta z)^{-2}\}$$

Instead of explicitly determining a new nodal value in terms of four neighbouring values at the previous time-step, the Dufort–Frankel scheme of (11) requires the inclusion of the value of $H_{i,j}$ two time-steps earlier, i.e. it is a three-tier system. There are in fact two independent interleaved sets of nodal values of $H$ that can be pictured in terms of a

**Table 1: Impedance of disc at two frequencies**

| Frequency (MHz) | 0.25 | 0.25 | 0.25 | 0.5 | 0.5 | 0.5 |
|---|---|---|---|---|---|---|
| Radius(*m*) | *R* (Ω) | *X* (Ω) | \|*Z*\| Ω | *R* (Ω) | *X* (Ω) | \|*Z*\| Ω |
| 1.0 | 30.18 | 8.911 | 31.46 | 34.05 | 13.20 | 36.52 |
| 1.25 | 25.66 | 8.931 | 27.17 | 29.55 | 13.24 | 32.38 |
| 1.5 | 22.59 | 8.933 | 24.29 | 26.49 | 13.25 | 29.62 |

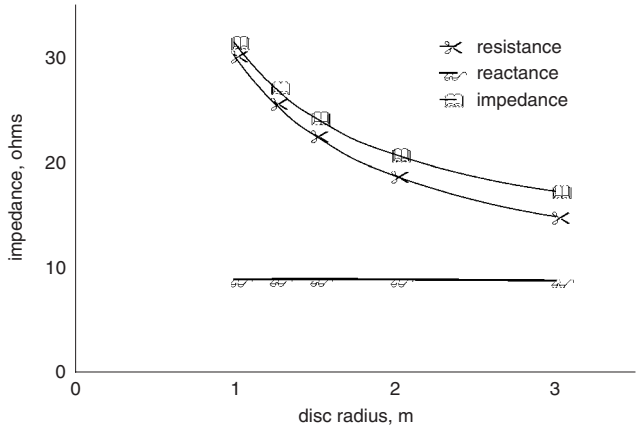


**Fig. 3** *Resistance and reactance of surface disc of increasing radius operating at 0.25 MHz*

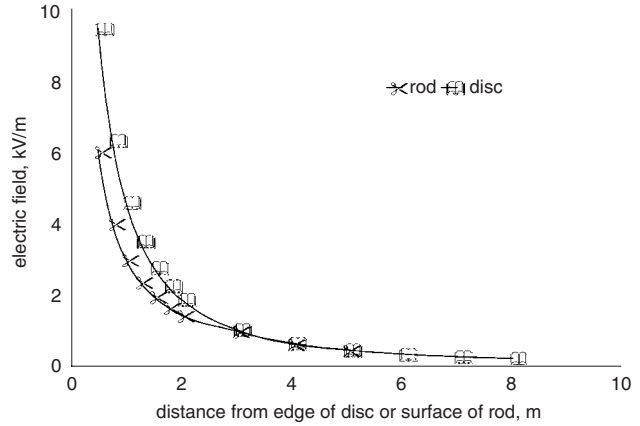


**Fig. 4** *Variation of magnitude of surface electric field with distance from 5 m vertical rod and edge of horizontal 1 m radius disc when steady-state current of peak value 1000A is injected at 0.25 MHz*

three-dimensional 'chess board' consisting of black and white nodes in a space–time continuum.

Application of the boundary conditions follows the complex case. The excitation appears in the boundary (ground surface) term $i(t)/2\pi$, where the current is now a specified function of time. Three models of a transient current pulse were used, all having a peak value of 1000A.

- Half sinusoids of width 1 and 2 $\mu$s, i.e. with rise times of 0.5 and 1 $\mu$s.
- Triangular waveforms with steep wavefronts rising linearly for 0.5 and 1 $\mu$s, followed by a long tail of 100 $\mu$s. Only a short section of the latter was computed because the sudden change of slope makes this waveform very artificial.
- A standard double-exponential impulse of the form $i=\beta\{\exp(-\alpha_1 t)-\exp(-\alpha_2 t)\}$. The shortest one recommended by IEC 1989 [9] is the 1/20 pulse with a front time $T_1=1\,\mu$s and a time-to-half-value $T_2=20\,\mu$s; $T_1$ is defined as 1.25 $T$, where $T$ is the time taken for the current to rise from 10 to 90% of its peak value; $T_2$ is the time from the start of the impulse to the instant at which the current tail has decreased to half the peak value. To achieve these times and a peak of 1000A, it is required that $\beta=1086$, $\alpha_1=3.65\times10^4$ and $\alpha_1=2.3\times10^6$. The current changes relatively slowly near its peak value, the latter only being reached after 1.8 $\mu$s. However, the magnitude of the current at $t=T_1$ is 940A, which is sufficiently close to 1000A to enable reasonable comparison with other model risetimes of 1 $\mu$s.

The minimum space step employed was 0.02 m and the soil conductivity assumed to be 0.01 S/m. If (10) is interpreted as requiring $\Delta t/0.02$ (where $\Delta t$ is expressed in seconds) to be 100 times less than $\sqrt{(\sigma\mu_0)}$, the maximum time-step is only 0.02 $\mu$s. The latter value can be used during the tail of the pulse, but after some experimentation $\Delta t$ was set 100 times smaller for the initial rise.

## 5 Transient results

A current impulse in the form of half a sine wave can be used as a convenient check on the transient computer program. With a pulse of width 1 $\mu$s, a peak potential of 37.12 kV occurred on the rod after 0.34 $\mu$s, or 0.16 $\mu$s before the current peak. In contrast, the 0.5 MHz steady-state peak is 39.01 kV with the current phasor lagging the voltage by 31.1°, or 0.173 $\mu$s (using the 0.5 MHz impedance quoted in Section 3). The time displacements are within 8% and the peak impulse potential is 5% lower than its steady-state counterpart. For a pulse of 2 $\mu$s width, i.e. 1 $\mu$s rise, the latter difference is about 3.5%. However, one should not expect complete agreement because the half-sinusoid is a transient impulse and not simply a segment of a steady-state excitation process.

Table 2 gives the results for two triangular current pulses, together with the peak value of the steady-state voltages at the corresponding frequencies. The maximum potential always occurs at the end of the rise period in this simplified linear model. The steady-state results appear to underestimate the maximum impulse potential by between 6 and 8%.

**Table 2: Peak potentials on 5 m rod subjected to triangular pulse of 1000A peak**

| Risetime ($\mu$s) | Maximum potential (kV) | Time at which peak occurs ($\mu$s) | Steady-state peak potential (kV) |
|---|---|---|---|
| 0.5 | 41.55 | 0.5 | 39.01 |
| 1.0 | 34.38 | 1.0 | 31.71 |

A more informative result is found in Fig. 5 where the double-exponential 1/20 current impulse and its potential rise response are shown over a period of 1.7 $\mu$s. The peak voltage is 27.4 kV and occurs at $t\approx0.9\,\mu$s. The triangular

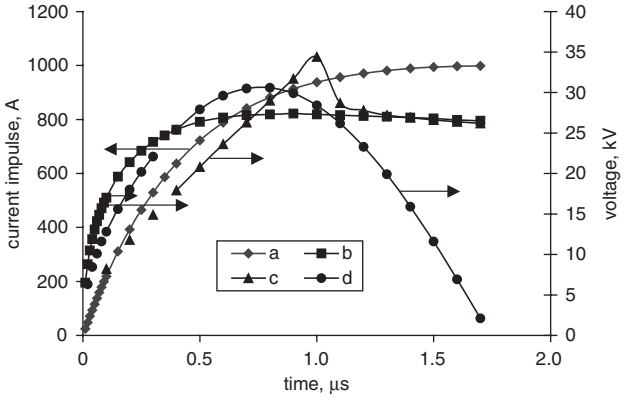


**Fig. 5** *Potential of 5 m rod subjected to current impulses with approximately 1 $\mu$s rise times*
*a* Double-exponential impulse current
*b* Double-exponential potential
*c* Triangular (linear) potential
*d* Half-sine potential

and sinusoidal impulse voltage responses are also superimposed on Fig. 5, both for 1 $\mu$s risetimes. Over the first 0.5 $\mu$s the exponential and sinusoidal potential values are similar. Thereafter, as might be expected, there is no agreement. However, the potential associated with the linear impulse decays sharply after its peak value of 34.4 kV and merges with that of the exponential impulse while the latter is still close to its maximum of just over 27 kV. This is due to the fact that the rates of change of both currents are small in this region.

It was noted with reference to Table 2 that the steady-state solutions produce peak voltages that are approximately 7% lower than the values obtained from the linear impulses. On the other hand, the 0.25 MHz solution yields a peak value about 15% higher than that of the double-exponential current impulse with a front time of 1 $\mu$s. However, the actual risetime of the latter is appreciably more than the front time and so comparison is difficult.

## 6 Conclusions

A typical 5 m high-frequency vertical earthing rod in homogeneous soil of conductivity 0.01 S/m has an AC impedance to DC resistance ratio of about 1.47 at 0.25 MHz (the lower end of the range normally assumed to represent lightning strikes). This ratio is approximately proportional to the square root of the soil conductivity. The high impedance is caused by the well-known skin effect, whereby all the current flows close to the surface. Not only is the resistance significantly increased above its low-frequency or DC value, but there is a substantial reactive component. Although the impedance can be reduced by making the rod longer, the gain becomes increasingly marginal. However, it has been shown that a horizontal disc on or just below the surface can be used as a successful alternative to the rod. Apart from the larger size, the only disadvantage of the disc is that the step potential close to its edge is higher than that of the vertical rod. The resistance can be reduced by increasing the radius of the disc as Fig. 3 illustrates if space allows, although in practice it would no doubt be preferable to bury the disc a short distance below the surface, which will have a similar, although less marked, effect that should be investigated. Of particular importance, the present study has shown that there is a significant reduction in the reactive component when two electrodes having the same DC resistance are compared. The disc reactance is found to be independent of radius.

By solving the rod problem in real time using triangular and double-exponential current impulses with appropriately steep wavefronts, the practice of employing a steady-state frequency to represent a lightning impulse has been shown to be a reasonable one.

## 7 Acknowledgments

The authors are grateful to NGC for the award of a grant that enabled this work to be done and for giving permission for publication.

## 8 References

1 Stoll, R.L.: 'Analysis of eddy currents' (Clarendon Press, Oxford, 1974), pp. 10–23
2 Sykulski, J.K.: 'Computational magnetics' (Chapman & Hall, London, 1995)
3 http://www.vectorfields.co.uk accessed 13 May 2003
4 Geri, A.: 'Behaviour of grounding systems excited by high impulse currents: the model and its validation', *IEEE Trans. Power Deliv.*, 1999, **14**, (3), pp. 1008–1017
5 Stoll, R.L.: 'Solution of linear steady-state eddy-current problems by complex successive over-relaxation', *Proc. Inst. Electr. Eng.*, 1970, **116**, pp. 1317–1323
6 Carre, B.A.: 'The determination of the optimum accelerating factor for successive over-relaxation', *Comput. J.*, 1961, **4**, pp. 73–78
7 Burden, R.L., and Faires, J.D.: 'Numerical Analysis' (Brooks/Cole, Pacific Grove, 2001), p. 171
8 Dufort, E.C., and Frankel, S.P.: 'Stability conditions in the numerical treatment of parabolic differential equations', *Math. Tabl Natl. Res. Counc., Washington*, 1953, **7**, pp. 135–152
9 BS 923-1 1990, 'High-voltage testing techniques', Part 1 General, pp. 34-36, 62 or IEC Standard 60-1: 1989, Section 8: 'Tests with impulse current'